Shielding effects in multiple fatigue cracks: an experimental simulation of thermal fatigue effects, in stainless steel 304

A. Köster[1, a], M. Dib[1,b], L. Rémy[1,c] and C. Amzallag[2,d]

[1]Mines ParisTech, Centre des Matériaux, CNRS UMR 7633, BP 87 F-91003 Evry Cedex, France

[2]EDF-Septen, 12-14 avenue Dutriévoz, F-69628 Villeurbanne Cedex, France

[a]alain.koster@ensmp.fr, [b]mustapha.dib@ensmp.fr , [c]luc.remy@ensmp.fr , [d]claude.amzallag@edf.fr

Abstract. This paper investigates the harmfulness of cracks networks using both experiments and finite element analysis. A single array of parallel cracks with a central deeper notch and regularly spaced secondary notches of identical depth is used to investigate crack arrest under fatigue loading. Tests are carried out on 304 stainless steel using a load shedding program prescribed as a function of central crack depth; this loading program is deduced from the numerical analysis of thermal fatigue cracks, in EDF components. The difference in length between the dominant crack and secondary cracks is varied to identify conditions giving rise to crack arrest. Fatigue crack growth results are rationalized using finite element computations of stress field using a visco-plastic constitutive model.

Introduction

Thermal fatigue crack network have been found in various components of nuclear power plants, in particular in auxiliary loops of primary cooling systems in Pressurized Water Reactors (PWRs). The evolution of the mixing boundary between hot and cold water causes temperature fluctuations at the inner surface of the pipes (in horizontal section, t-junctions of connected lines to main loops). This can give rise to thermal fatigue in pipes mainly made from 304L stainless steel (base metal or welds). The nucleation of fatigue cracks is investigated using thermal shock experiments [1-3] or thermal mechanical fatigue tests [4-6]. Thermal shock experiments are used to investigate crack growth and the development of the crack network [7, 1-3]: usually the crack network tends to stabilize and the growth rate of the deeper cracks tends to slow down but experiments can only be completed for a few hundred of thousand cycles. In service hundred of millions cycles and more are of interest that cannot be investigated directly under thermal shock conditions.

A major concern in service conditions is to assess if such complex thermal fatigue cracks networks yield to crack arrest or if a crack may become critical due to uncertain boundary condition. Shielding effects in crack networks have stimulated already finite element computation of simple crack arrays [7, 8]. However direct experimental demonstrations are still lacking.

The purpose of this paper is to present an experimental investigation of shielding effects using a simple array of parallel cracks, under isothermal fatigue loading on 304 stainless steel. Previous thermal-mechanical fatigue experiments [4] suggest that for this alloy and the moderate temperature ranges under concern, thermal fatigue can be considered essentially as equivalent to an isothermal fatigue process. Therefore one may achieve large numbers of cycles using tests at higher frequency to investigate crack arrest conditions. A numerical fracture mechanics analysis has been carried out by EDF for a thermal loading spectrum in actual components. This analysis has led to the definition of a load shedding program as a function of a single crack depth. This load shedding program was applied to different crack configurations, a single crack and a dominant crack within parallel secondary cracks. The difference in depth between the dominant crack and secondary cracks was

varied to identify the conditions giving rise to crack arrest. These results are discussed using finite element computations of stress-strain fields and infrared thermo-graphic measurements.

Material and experimental details

A 304L austenitic stainless steel was used in the study with chemical composition as follows (wt.%): C 0.029, Mn 1.86, Si 0.37, Cr 18.00, Ni 10.00, Mo 0.04, P. 0.029, S 0.004, Cu 0.02, N 0.056, Fe bal. as in previous work [4].

Fatigue crack growth tests were carries on single edge notch tensile specimens (SENT) using the same geometry as in earlier investigations on short cracks in superalloys [9]. Specimen heads are compatible with a standard gripping system for cylindrical LCF tests (nominal diameter 18mm in the fillet). The central part is 20mm in gage length, 18mm wide and 4mm thick. The central edge notch is machined using electro-discharge machining. This ensures a high degree of constraint and the calibration of the compliance function Y(a/w) has been reported elsewhere [9, 10].

Tests using a single edge notch were carried out at 25°C at 20Hz frequency. Reference curves were conducted using a constant load ratio R = K_{min}/K_{max}, either 0.1 or 0.7. Most tests were carried out using a special load shedding program prescribed as a function of crack depth: this loading was deduced from a numerical fracture mechanics analysis of thermal fatigue cracks in components that was made by EDF. The evolution of K_{max}, K_{min}, and ΔK used is shown in Fig. 1. ΔK is decreased slowly with increasing crack length from 1mm to 5mm and simultaneously K_{max}, is increased. This means a strong increase in the R ratio up to 0.8 at low ΔK values.
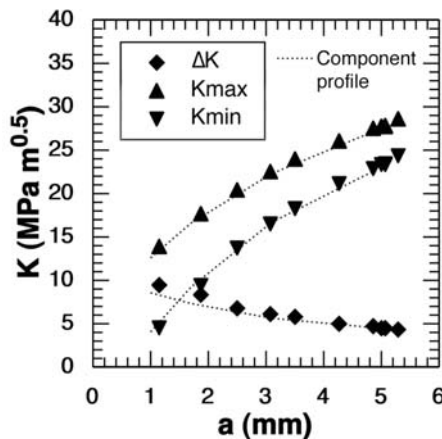

Fig. 1. Variation of maximum (resp. minimum) value and range of stress intensity factor, as a function of crack depth (dotted curves correspond to expected evolution, and solid points to achieved experiments).

Load shedding was done using a manual procedure: a potential drop technique was used to monitor crack growth and optical measurements were made directly at test interruptions to calibrate "in situ" the potential drop measurements. The load was decreased at least after every 0.2mm crack growth.

Similar tests were carried out on the same specimen type but using a crack array instead of standard SENT geometry. An array of 7 parallel notches with a constant spacing, 2mm as deduced from the observations of real thermal fatigue crack networks, was used with a central deeper notch. The behavior of the crack emanating from the central notch was compared with that of SENT specimens. The difference in notch depth between the central crack, simulating a dominant crack within a real thermal fatigue network, and secondary notches (of same depth) was varied to identify

17th European Conference on Fracture
2-5 September, 2008, Brno, Czech Republic

ECF17
ECF17

BRNO '08
IX 2 - 5

conditions giving use to crack arrest. A typical parallel array of notches is shown in Fig. 3. The same load shedding program was applied for the specimens with an array of notches as for a single crack.

In order to understand experimental crack growth rate curves, a few measurements were made using a thermo-graphic camera and dedicated software. Finite element analysis using Zebulon software was made to analysis fatigue crack growth results. Computations of the stress intensity factors were done first using the methods proposed by Parks and Hellen [11, 12]. Stress-strain fields at the crack tip were computed using standard plane strain or plane stress approximations. The non-linear behavior of 304L stainless steels was described using a standard Chaboche visco-plastic model with non-linear kinematic hardening [13]. Parameters identified in a previous investigation [14, 6] were used.

Results

Single crack. The fatigue crack growth rate is plotted as a function of the range of stress intensity factor for a single edge notch situation in Fig. 2. The curve for a standard constant load ratio R = 0.1 displays a Paris type behavior with a constant m about 4 and a threshold in ΔK range 5-6 MPa m$^{1/2}$.
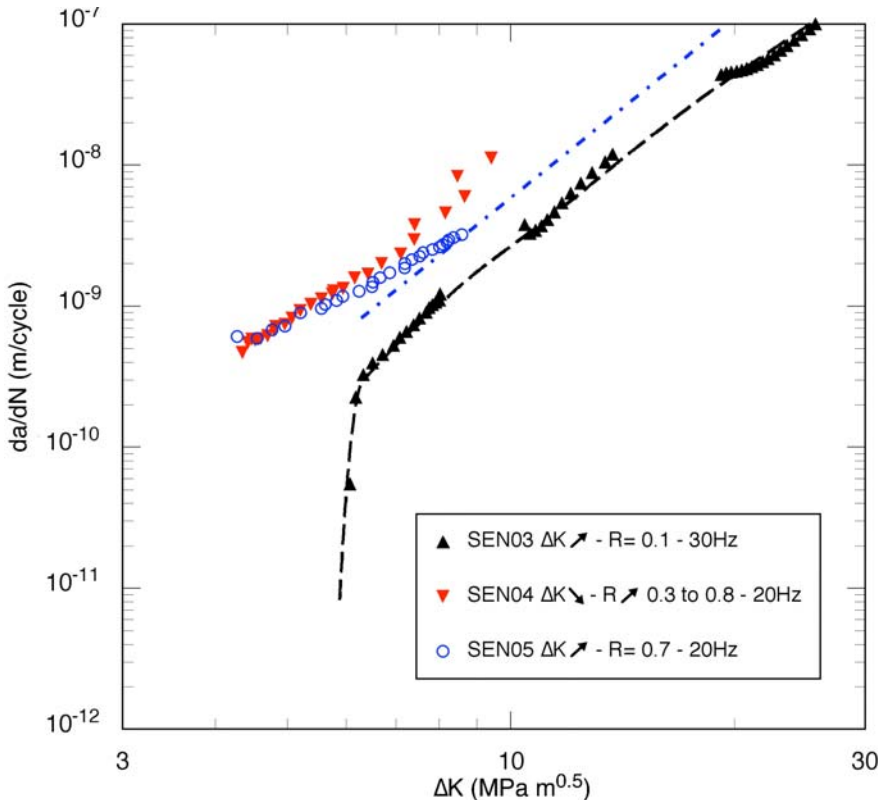

Fig. 2. Variation of fatigue crack growth rate as a function of the range of stress intensity factor. Curves for constant load ratio R 0.1 or 0.7 and experimental points for the prescribed load programme (increasing R from 0.3 to 0.8).

The load shedding program was used as shown in Fig. 1. The variation of K_{max} and ΔK as function of crack depth was achieved as expected from the initial analysis. A similar slope near 4 was found with decreasing ΔK but no threshold was observed down to $\Delta K = 3.8 MPa^{1/2}$ (see Fig. 2). In order to clarify this observation, a test was conducted at decreasing ΔK under a constant load ratio R = 0.7. A growth law was observed with a smaller slope (m = 2.6) but at low ΔK, the fatigue crack growth rates were almost identical between the load shedding program used in Fig. 1 and constant R = 0.7 results, with no threshold behavior for the lowest ΔK values used.

Crack array. The array of parallel notches of 2mm constant spacing is shown in the sketch of Fig. 3. The initial depth of the central notch a_c was kept constant about 1.65 or 1.6mm. Specimens were used with different depth a_s of secondary notches 0.65mm (specimen M01), 1.2mm (specimen M02) and 1.4mm (specimen M03); the difference in notch depth a_c - a_s varies as 1mm, 0.4mm and 0.2mm respectively.

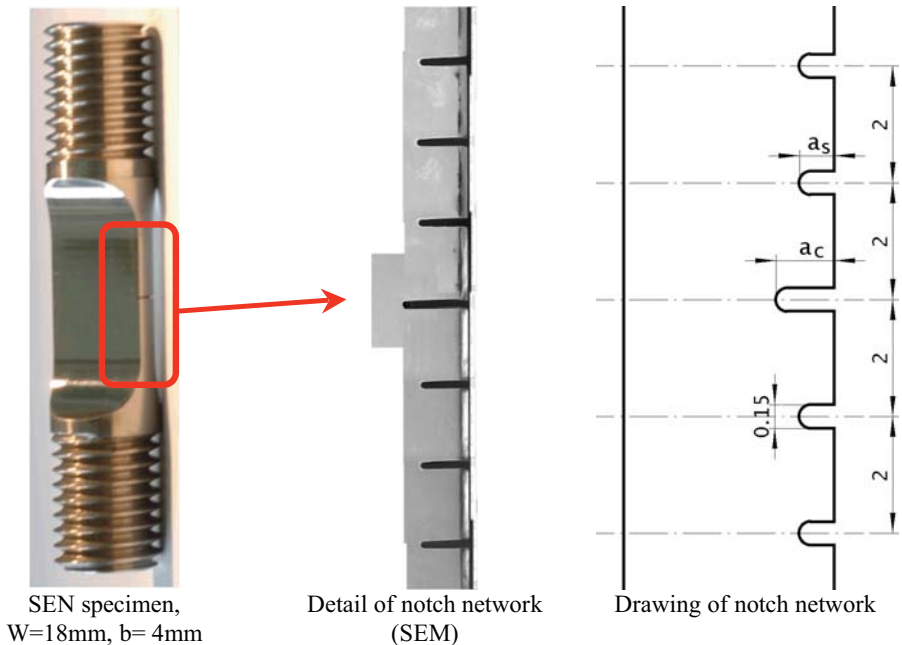| SEN specimen, W=18mm, b= 4mm | Detail of notch network (SEM) | Drawing of notch network |

Fig. 3. Specimen used for testing a parallel crack array: general view, detailed view of a notch network, sketch of crack array (all dimensions in mm).

The growth rate of the crack growing from the central notch is shown as a function of nominal ΔK, i.e. the value corresponding to a single crack submitted to the same load applied to the specimen, in Fig.4. There is more scatter in measurements for a notch array than for a single crack due to potential drop interferences due to secondary cracks. For secondary notches 0.65 mm deep, there is a significant shielding effect at initial ΔK values that vanishes for ΔK about 5 MPa.m$^{1/2}$. Very small cracks nucleated from secondary notches.

The initial shielding effect is much stronger for a secondary notch depth of 1.2 mm. The crack growth rate of the central crack stays constant until the shielding effect disappears at ΔK about 6 MPa.m$^{1/2}$.

When the depth of secondary notches a_s is 1.4 mm, the shielding effect is larger and only 30 µm crack growth is observed after 2 millions cycles resulting in a growth rate less than 2 10^{-11} m/cycle, typical of a threshold behavior.
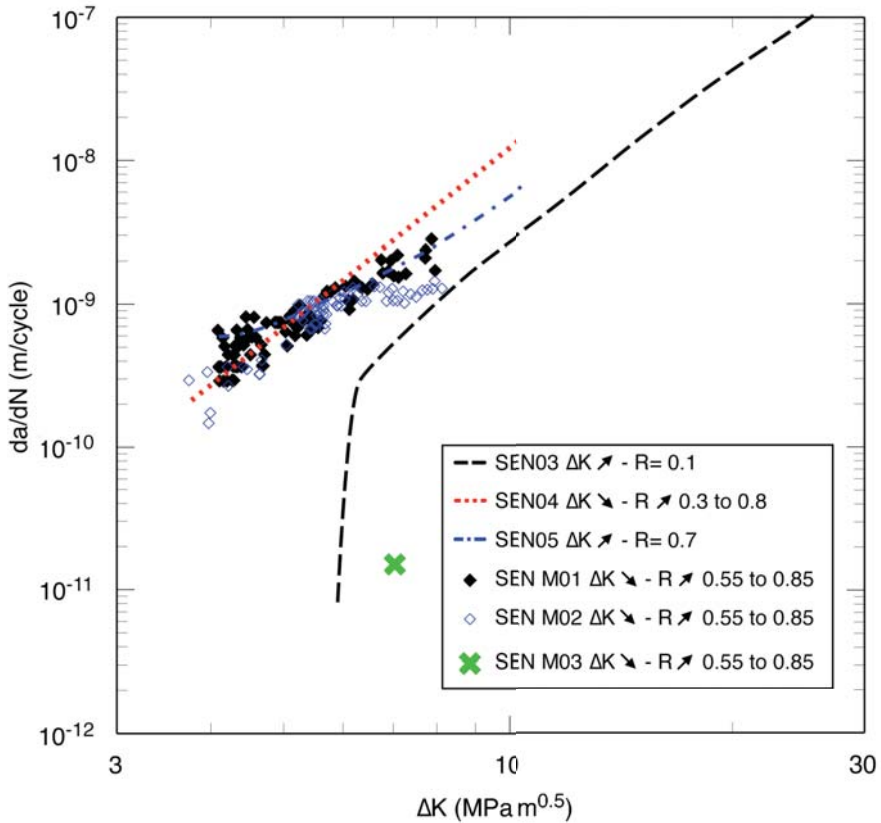
Fig. 4. Variation of fatigue crack growth rate as a function of the range of stress intensity factor: reference curves for a single crack with constant load ratio R 0.1 or 0.7 and prescribed load programme (increasing R from 0.3 to 0.8). Experimental points refer to the different notch arrays investigated (increasing R from 0.55 to 0.85).

Discussion

A finite element analysis was carried under a 2D plane strain approximation to estimate the stress intensity factor for single crack situations and multiple crack situations. For sake of conciseness only a few results are shown here (furthers details will be given in a forthcoming publication). The numerical procedure used was validated against previous results from literature for SENT specimens [15]. The comparison is shown in Fig. 5 for free rotation and clamped boundary conditions as well as for our specific SENT configuration.
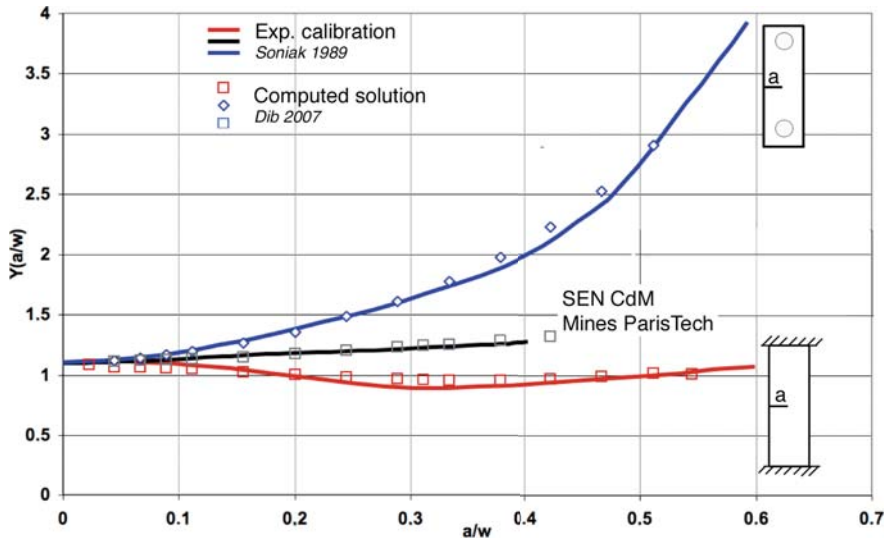
Fig. 5. Variation of compliance function Y(a/w) for single edge notch specimen with different boundary conditions (ends free in rotation, clamped ends, present specimen): points for the present computations, solid curves for previous results.

The procedure was then used for the various parallel notch arrays used in the experiments. The effective compliance function for the central crack was then computed and provides a complete tool to analysis the shielding effect. The effect can be illustrated more easily when looking at the stress strain field at the crack tip. Maps of von Mises stress at maximum load are shown for the initial notch arrays in Fig. 6.

SEN M01 a_c=1.65, a_s= 0.75
σ_{max}= 274.9 MPa
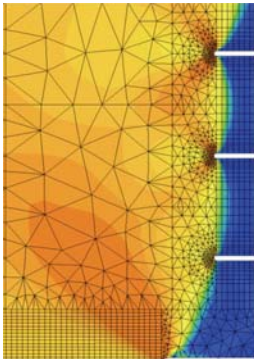
SEN M02 a_c=1.65, a_s= 1.25
σ_{max}= 270.1 MPa
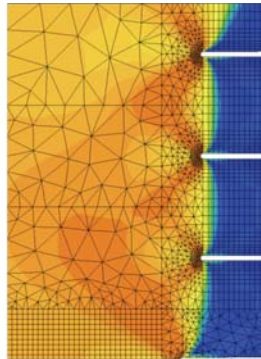
SEN M02 a_c=1.65, a_s= 1.45
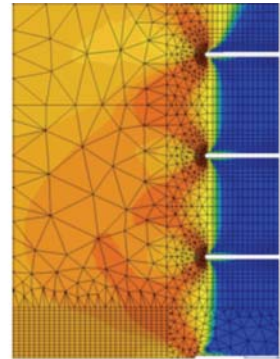σ_{max}= 257 MPa

Fig. 6. Maps of von Mises stress for various notch arrays submitted to the same loading conditions: central crack 1.65 mm deep and secondary cracks 0.65 mm deep, 1.25 mm deep and 1.45 mm deep (only upper half of the specimen is shown).

When the secondary notch depth is small (0.65mm) the central notch gives rise to a strong stress concentration and a large plastic zone. When the secondary notch depth is increased up to 1.2mm

and then 1.4mm the plastic zones of secondary notches increase and both the stress concentration and plastic zone size of the central notch strongly decrease.

The shielding effect was also confirmed experimentally using thermo-graphic measurements. A single example is shown in Fig. 7 for the central crack in specimen M02 where measurements are converted into maps of von Mises stress using a thermo-elastic analysis. This compares fairly well with plane stress computations of von Mises stress at the crack tip.
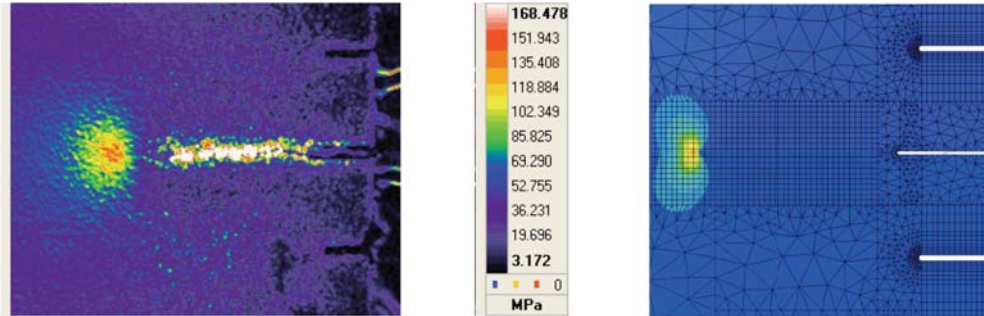

Fig. 7. Specimen M02: Maps of von Mises stress directly deduced from thermo-graphic measurements (left) and obtained from plane stress finite element computations (right).

Conclusions

This study of fatigue crack growth at room temperature in 304 stainless steel has shown that a single crack submitted to load shedding program as function of crack length (with increasing R ratio from 0.3 to 0.8) exhibits significant crack growth rates down to $\Delta K = 3.8 MPa^{1/2}$ with no crack arrest.

An array of parallel secondary cracks around a dominant crack gives rise to a shielding effect on the growth rate of the dominant crack. This shielding effect increases when the difference in crack depth between the dominant notch and secondary notches decreases from 1mm to 0.2mm. Crack arrest can be observed in the later condition.

A numerical computation of stress intensity factors can assess the decrease of effective K of the dominant crack due to the secondary crack array. Computation of the stress field using a viscoplastic constitutive model has shown the decrease in local stress concentration ahead of the main central notch.

Acknowledgements

References

[1]   D.J. Marsh: Fatigue of Engineering Materials and Structures, vol. 4 (1981), p.1179.

[2]   A. Fissolo, B. Marini, A. Berrada, G. Nais and P. Wident, Initiation and growth of cracks under thermal fatigue loading for a 316L type steel, Fatigue under thermal and Mechanical loading, J. Bressers and L. Rémy, Eds., Kluwer, Dordrecht, (1996), p. 67.

[3]   V. Maillot, A. Fissolo, G. Degallaix, S. Degallaix, S. Degallaix, B. Marini, M. Akamatsu, in : Temperature-Fatigue Interaction, L. Rémy and J. Petit (Eds.), ESIS Publication 29, Elsevier (2002), Amsterdam, p.135.

[4] N. Haddar, L. Rémy, A. Koster, M. Akamatsu, in: Fatigue 2002, 8th International Fatigue Congress, Stockholm, Sweden, 3-7 June 2002, Proceedings, A. F. Blom Ed., EMAS, Cradley Heath, UK, vol.3 (2002), p. 1665.

[5] L. Rémy, in: Comprehensive Structural Integrity, I. Milne, R. O. Ritchie and B. Karihaloo, Eds., vol. 5 Creep and High-Temperature Failure (vol. ed. A. Saxena), Elsevier, Amsterdam (2003), p. 113.

[6] L. Rémy, N. Haddar, A. Alam, A. Koster, N. Marchal: Materials Science and Engineering A, 2007, doi: 10.1016/j.msea.2006.08.133.

[7] A. Fissolo and B. Marini, in: Fracture from Defects, ECF 12, Proc. 12th Conference on Fracture, M.W. Brown, E. R. de Los Rios and K. J. Miller, Eds., EMAS, vol. I (1998), p. 31.

[8] M. Seyedi, F. Hild, S. Taheri, in: Fatigue 2002, 8th International Fatigue Congress, Stockholm, Sweden, 3-7 June 2002, Proceedings, A. F. Blom, Ed., EMAS, Cradley Heath, UK, vol.3, p. 1735.

[9] F. Soniak, L. Rémy, in: The behaviour of short fatigue cracks, K.J. Miller and E.R. de Los Rios, Eds., EGF Publication 1, Mechanical Engineering Publications, London (1986), p.133.

[10] F. Soniak, "Propagation des fissures courtes en fatigue dans un alliage pour disques de turbomachines", PhD Thesis, Ecole des Mines de Paris, 1989.

[11] D. Parks: Int. Journ. of Fract. Mech., vol. 10 (1974), p. 487.

[12] T.K. Hellen: Int. Journ. of Num. Meth. In Eng., vol. 9 (1975), p. 187.

[13] J.L. Chaboche: Int. Journ. of Plasticity, vol. 5 (1989), p. 247.

[14] N. Haddar, « Fatigue thermique d'un acier inoxydable austénitique 304L : simulation de l'amorçage et de la croissance des fissures courtes en fatigue isotherme et anisotherme », Ph D Thesis, Ecole des Mines de Paris, 2003.

[15] J.M. Bloom: Int. Journ. of Fract. Mech., vol. 2 (1966), p. 597.